Time-Dependence of an Atomic Electron Wave-Function in an Electrical-Field

Noordam, L.D.; Tenwolde, A.; Lagendijk, A.; Vandenheuvel, H.B.V.

DOI
10.1103/PhysRevA.40.6999
Publication date
1989

Published in
Physical Review A. General Physics

Time dependence of an atomic electron wave function in an electrical field

L. D. Noordam and A. ten Wolde
Foundation for Fundamental Research on Matter (FOM)–Institute for Atomic and Molecular Physics, Kruislaan 407, 1098 SJ Amsterdam, The Netherlands

A. Lagendijk
Foundation for Fundamental Research on Matter (FOM)–Institute for Atomic and Molecular Physics, Kruislaan 407, 1098 SJ Amsterdam, The Netherlands and Natuurkundig Laboratorium of the University of Amsterdam, Valckenierstraat 65, 1018 XE Amsterdam, The Netherlands

H. B. van Linden van den Heuvell
Foundation for Fundamental Research on Matter (FOM)–Institute for Atomic and Molecular Physics, Kruislaan 407, 1098 SJ Amsterdam, The Netherlands

(Received 7 June 1989; revised manuscript received 23 August 1989)

We present measurements and calculations of the time-dependent behavior of an electron bound in a Coulomb potential placed in an additional static electrical field. The time-dependent behavior is studied by means of the evolution of a wave packet. The wave packet is created by coherent superposition of several k states of one Stark manifold. It is pointed out that the oscillation of this "parabolic" wave packet corresponds to an oscillation of the angular momentum l. In the case of a hydrogen atom the spacing between the k states is constant, leading to a dispersion-free wave packet. For this situation the parabolic wave packet $|\Psi(x,z)|^2$ is plotted as a function of time. The oscillations of the parabolic wave packet can be measured by photoionization, because the photoionization probability is l dependent. The time-dependent photoionization probability is calculated in two steps. First the l-population coefficients are calculated as a function of time. Then we calculated the transition probability of each l state to the continuum. Combining these two allows us to calculate the time-dependent ionization probability. Experimentally, a wave packet is created by coherent superposition of k states of rubidium atoms with a 7-ps laser pulse. The ionization probability is probed by a second laser pulse, which is delayed with respect to the first one. In this way as many as ten oscillations of the parabolic wave packet are observed. The calculations (for hydrogen) agree well with the experimental result of the pump-probe experiment. The ac Stark shift of a k manifold due to the laser field was measured in a separate experiment; the determined value of 0.01 meV/(GW/cm^2) is low enough to ensure that intensity effects can be neglected.

I. INTRODUCTION

Coherent superposition of eigenstates of a quantum system leads to some kind of localization of the wave function. The concept of this so-called wave packet is as old as quantum mechanics itself.[1] As a result of new experimental possibilities, there is a renewed interest in the theory of wave packets. Radially localized atomic electrons are described by a superposition of Rydberg n states,[2,3] whereas atomic electrons localized in the angular directions are described by coherent superposition of l,m states.[4] Previously, we reported[5,6] on the observation of a radially localized wave packet created and detected with ps laser pulses. These radial wave packets spread out after several oscillations, because of the varying spacing between the energy levels. After about $n/6$ oscillations the radial wave packet is fully spread out.[7] The reported wave packet localized in the angular directions also disperses. In that case the energy splitting of the m states is not constant. To create a wave packet with less dispersion a quantum system with a more constant energy spacing between the energy levels should be used.

If an atom is placed in a static electrical field the energy levels are split and shifted. For a hydrogen atom in a small electrical field the energy levels are given by $Enk=-1/2n^2+\frac{3}{2}Fnk$ (atomic units are used throughout this paper) where n is the principal quantum number and k the parabolic quantum number. The spacing between subsequent energy levels is $\Delta E=3Fn$. Since the spacing is k independent there is in principle no dispersion. Coherent excitation of the k states will lead to the formation of a wave packet. The oscillation time of this wave packet is

$$\tau=\frac{2\pi}{3Fn} . \tag{1}$$

Recently we reported[8] on the observation of atomic electron wave packets in an electrical field. In this paper we will give a more detailed description of both theory and experiment. The problem of an atom in an electrical field has been studied extensively in the frequency domain (e.g., Refs. 9 and 10). In this paper we present a time-resolved spectroscopy study. We like to point out the

connection with other studies of quantum-beat phenomena: In the limit of low principal quantum number our approach becomes equivalent with the observation of coherent effects in beam-foil spectroscopy.[11] With this technique the observed signal is due to radiative decay, while in this paper photoionization is used to probe the population coefficients. The slow radiative decay in the visible range limits the time resolution to nanoseconds or longer. In the case of photoionization the resolution is given by the duration of the laser pulse, which can be on a femtosecond time scale.

The paper is organized as follows. First we will present a quantum-mechanical description of the evolution of the parabolic wave packet (Sec. II); eventually the time-dependent photoionization is calculated in Sec. III. The setup used for the experiments is described in Sec. IV. In Sec. V the experimental results are presented and compared with the quantum-mechanical calculations. Finally we come to conclusions in Sec. VI.

II. CREATION AND EVOLUTION OF THE WAVE PACKET

If a hydrogen atom in an electrical field is excited with a short laser pulse, the resulting wave packet is a coherent superposition of the so-called parabolic states.[12] These states are the eigenstates of an atom in an electrical field, and they are labeled with the quantum numbers n_1, n_2, the parabolic quantum numbers, and m, the azimuthal quantum number. The electronic motion is separable in the parabolic coordinates, $\xi=r+z$, $\eta=r-z$, and ϕ. The eigenfunctions are analytically known. If only parabolic states within one n manifold are excited, we can use n, k, and m as quantum numbers, where $k=n_1-n_2$. So in an electrical field the angular momentum l is not conserved but the electrical dipole moment connected to the quantum number k is. We study the time dependence of an atomic electron in an electrical field by the evolution of the wave packet. This wave packet can be written in terms of k states, but since a movement of the wave packet corresponds to an oscillation of the angular momentum, the l basis can also be useful:

$$\Psi(\mathbf{r},t)=\sum_k a_k e^{i\omega_k t}|k\rangle=\sum_l c_l(t)|l\rangle \ , \tag{2}$$

where a_k are the population coefficients of the k states, $\omega_k=-1/2n^2+\frac{3}{2}Fnk$ the energy levels, and $|k\rangle$ the parabolic eigenstates, while $c_l(t)$ are the time-dependent amplitudes of the l states and $|l\rangle$ the eigenstates of the angular momentum l. Since the functions $|k\rangle$ are the eigenfunctions of the Hamiltonian, in the k basis the time dependence is fully described by the phase factor $\exp(i\omega_k t)$, while the population coefficients are constant in time. In the l basis, this is no longer the case: the fact that the angular momentum l is not a conserved quantity in an electrical field is reflected in the time-dependent populations of the different l states. We can write down an expression for this time dependence as follows:

$$c_l(t)=\sum_k e^{i\omega_k t}a_k b_{lk} \ , \tag{3}$$

where[13]

$$b_{lk}\equiv\langle l|k\rangle = (-1)^m\sqrt{2l+1}\begin{pmatrix}(n-1)/2 & (n-1)/2 & 1\\ (m-k)/2 & (m+k)/2 & -m\end{pmatrix} \tag{4}$$

are the transformation matrix elements, which are the Clebsch-Gordan coefficients. The large brackets indicate the 3J symbols. The unitarian matrix is real. If we excite the k states with a Gaussian pulse of duration τ_p and central laser frequency ω_L, the population coefficients of the k states after the exciting pulse take the values

$$a_k=b_{k,l_0}e^{-(\omega_g-\omega_k+\omega_L)^2\tau^2/(2\ln 2)} \ , \tag{5}$$

where l_0 is the l state populated from the ground state (located at ω_g) as a result of the selection rules without electrical field. Using Eq. (3) we can now calculate the time evolution of the l populations. All the calculations in this section have been done for $n=8$, $F=300$ V/cm, $\tau_p=10.9$ ps. A low n value was chosen to keep the number of nodes in a picture of the wave function reasonable (as in Fig. 2). Assumed is that $l=0$ is populated from the ground state, and the central laser frequency coincides with the center of the manifold. In Fig. 1 the mean l value and the width (2σ) are plotted for the same calculation from $t=0$ to $t=1.2\tau$. The pulse duration has been chosen in such a way that the width of the packet remains as constant as possible during the oscillation. At the same time the mean l value changes from $l=0.2$ ($t=0$) to $l=6.5$ ($t=0.5\tau$), which are almost the minimum and maximum possible value. Directly after the pulse 92% of the population is in $l=0$. The leftover 8% is in $l=2$; since the pulse has a finite duration, some l mixing occurred already during the pulse. We see that in the quantum-mechanical calculations the electrical field induces indeed a beat in the l populations with a period of $\Delta\omega=\omega_k-\omega_{k-2}$. Note that if we had neglected the finite pulse duration of the laser pulse we would have obtained the known analytical

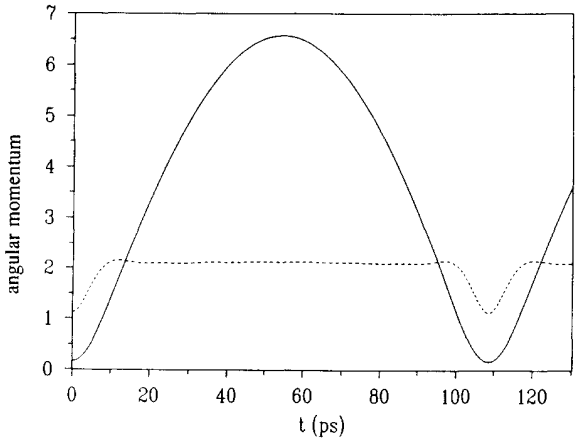

FIG. 1. Mean value of the l distribution (solid line) and the width (2σ) of the l distribution (dotted line) of the parabolic wave packet as a function of time. The calculation is done for $n=8$, $F=300$ V/cm, and a pulse duration of 10.9 ps.

result $l^2=\frac{2}{3}(n^2-1)\sin^2(\Delta\omega t/2)$ that can be derived, e.g., by writing the wave function on a basis where the sum and the difference of the angular momentum and the Runge-Lenz vector are diagonal.

The calculation of the time evolution of the wave packet is done for hydrogen. In the experiment we used rubidium. The low l states of rubidium have a large quantum defect, giving rise to deviations of the hydrogen model. First of all the position of the energy levels is affected by the states with a large quantum defect ($s-p-d$). The spacing between neighboring states is not constant anymore, leading to some dispersion of the wave packet. Furthermore the amplitudes of the different k states differ from the hydrogen case [Eq. (5)], since the states of the Stark map couple for rubidium. This will influence the time-dependent behavior of the wave packet.

Since Eq. (3) gives the population of the l states as a function of time, the time evolution of the wave packet in space can be calculated using Eq. (2). If the exciting pulse is linearly polarized in the direction parallel to the electric field (z axis), the selection rule is $\Delta m=0$, so only $m=0$ is excited from the ground state. In the absence of ϕ dependence we calculated the probability distribution $|\Psi(x,z)|^2$ for a given $n,m=0$ as a function of time [Figs. 2(a)–2(d)]. At $t=0$ the wave function has almost a pure s character which is strongly localized near $r=0$. At $t=18.1$ ps ($\frac{1}{6}\tau$), the wave function has split up in two peaks which move along the z axis away from the atomic core. Also, the formation of nodes in the θ direction is already visible. At $t=54.3$ ps ($\frac{1}{2}\tau$) the highest mean l value has been reached. The wave packet is localized in two peaks centered at $x=0$, $z=\pm n^2$, with $2n-4$ small side lobes at $r=n^2$ which are equally spaced in the θ direction, indicating that a wave function has the character of a wave function with high angular momentum.

III. PHOTOIONIZATION OF THE WAVE PACKET

In the case of a radially localized wave packet, photoionization was used as a tool to observe the oscillations of

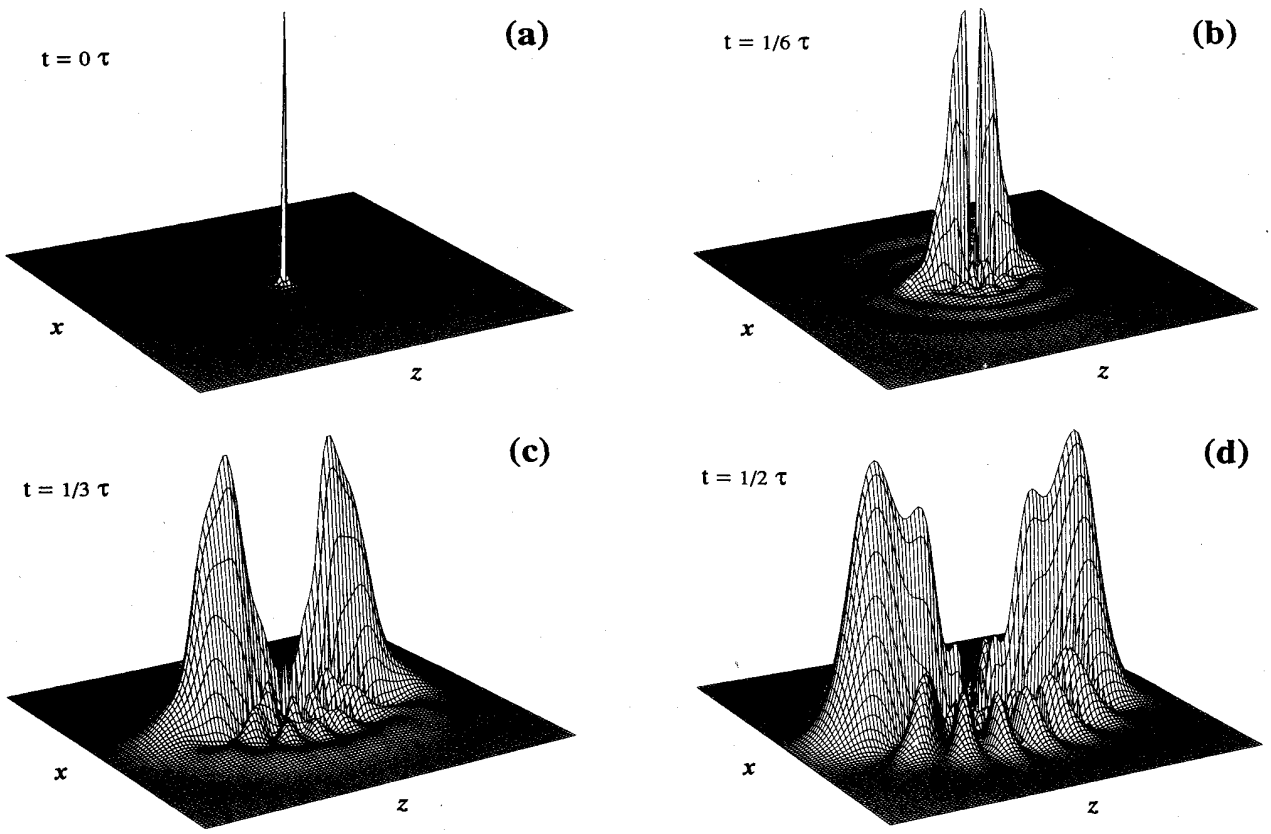

FIG. 2. The calculated probability distribution $|\Psi(x,z)|^2$ of the parabolic wave packet as a function of time. The vertical axis is scaled on the maximum value. In the xz plane the values of x and z lie between $-2.2n^2$ and $2.2n^2$. The wave packet ($n=8$) is created with a 10.9-ps pulse in an electrical field of $F=300$ V/cm. The function is symmetric around the z axis ($m=0$). Initially [(a) $t=0$] the $l=0$ character dominates: there is hardly any θ dependence and the wave function is strongly localized near the core. The number of nodes in the θ direction increases for longer times [(b) $t=\frac{1}{6}\tau$ and (c) $t=\frac{1}{3}\tau$]. There is almost no wave function near the core, indicating that the ionization probability is low. At $t=\frac{1}{2}\tau$, the wave packet has almost an $l=n-1$ distribution.

the wave packet. In order to show that this technique can also be applied to measure the oscillations of the parabolic wave packet, we have calculated the time dependence of the ionization of an atom in an electrical field. In general, the photoionization probability depends on the gradient of the potential,[7] ∇V. For a Coulomb potential, this means that the ionization probability goes at least with $1/r^2$, so that the absorption of photons leading to ionization is strongly peaked near $r=0$. The probability of finding the electron near $r=0$ decreases rapidly with increasing l. Therefore the quantum beat in the l populations (with period τ) leads to a periodically varying photoionization probability. This can also be calculated in the following way. For the initial and the final state we take

$$|\Psi_i\rangle = \sum_n \sum_l c_{nl}(t)|nlm\rangle \ , \tag{6a}$$

$$|\Psi_f\rangle = \int_0^\infty d\varepsilon \sum_{l'} c_{\varepsilon l'}(t)|\varepsilon l'm'\rangle \ , \tag{6b}$$

with ε the energy of the continuum state. We assume that we excite only one n state, so the summation over n in the initial state disappears. Now we can calculate the photoionization probability by a second laser pulse centered around t and with an intensity profile $I(t'-t)$. In first-order perturbation theory, adopting the rotating wave approximation, and neglecting depletion effects, the photoionization probability can be written as (compare, e.g., Ref. 14)

$$P_{\varepsilon,n}(t) \propto \int_{-\infty}^{\infty} dt' I(t'-t) \sum_l \left| \sum_{l'} a_{l'}(t') \mu_{nlm}^{\varepsilon l'm'} \right|^2 , \tag{7}$$

where

$$\mu_{nlm}^{\varepsilon l'm'} = \langle \varepsilon l'm'|r|nlm\rangle = \int_0^\infty dr\, r^2 R_{\varepsilon l'} r R_{nl} \int_0^{2\pi} d\phi \int_0^\pi d\theta \sin\theta Y_{l'm'} Y_{lm} \tag{8}$$

is the dipole matrix element. The integral over θ for $m=0$ and $m'=0$ gives the analytical result that $\langle Y_{l+1,0}|Y_{l,0}\rangle = (l+1)/\sqrt{(2l+3)(2l+1)}$. This integral hardly varies with l and is always of the order of $\frac{1}{2}$. The integral over r is responsible for the strong l dependence of the ionization probability with l. We calculated the integral numerically for a one-photon transition from a continuum state with $E=3\times10^{-5}$ eV (simulating a highly excited state) to a state 2 eV above the ionization limit. The simulation of the Rydberg state by a low-energy continuum state is particularly correct near the atomic core. For the calculation, only the wave function near the core is of importance, since only that part of the wave function contributes to the dipole matrix element. We calculated the Rydberg wave functions for the following potential:

$$V(r) = \frac{1+(Z-1)e^{-r/r_0}}{r} \ , \tag{9}$$

with Z the nuclear charge and r_0 a radius chosen in such a way that the quantum defects δ_l are generated as correctly as possible. The results for rubidium ($Z=37$, $r_0=0.394$) are shown in Table I. Finally an integral over the energy ε should be taken. However, this integral is strongly peaked around 2 eV, where the energy dependence of the photoionization probability is negligible.

TABLE I. Calculated radial matrix elements $M_{l,l'} = \int dr\, r^2 R_{\varepsilon l'm'} r R_{nlm}$ for a potential given in Eq. (9) that models rubidium. For the initial state $|nlm\rangle$ the principal quantum number was taken to be $n=\infty$, simulated by a continuum state with an energy of $E=27.2\times10^{-6}$ eV. The energy of the final $|\varepsilon l'm'\rangle$ state was 2.0 eV.

l	l'	$M_{l,l'}$
0	1	−0.18
1	0	−0.29
1	2	0.06
2	1	0.13
2	3	−0.02
3	2	−0.20
3	4	0.01
4	3	0.12
4	5	0.03

The ionization probability at time t can now be calculated in two steps. First we calculate the population coefficients of the different l states [Eq. (3)], then the ionization probability by Eq. (7). Such a calculation has been performed (Fig. 3) for the same parameters as used in the previous calculations: $n=8$, $F=300$ V/cm, while the excitation and ionization pulse have a duration of 10.9 ps. Note that this calculation of the evolution of the parabolic wave packet assumes that we study the evolution after the excitation pulse. The same holds for the ionization probability. Therefore $P(t)$ is meaningless for small values of t.

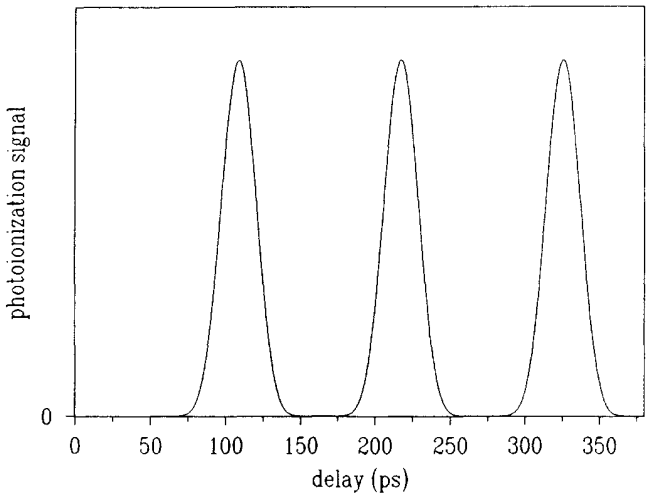

FIG. 3. The calculated ionization probability of a parabolic wave packet. The wave packet is again created with a 10.9-ps pulse ($n=8$, $F=300$ V/cm) and also detected with a 10.9-ps pulse. The ionization probability is high when the angular momentum of the parabolic wave packet is low, which occurs at an integer number of the oscillation time of 108.6 ps.

IV. EXPERIMENTAL SETUP

For the measurement of the time dependence of the ionization of atoms placed in an electrical field, we used a setup consisting of a laser system and a vacuum system. In order to generate the light pulses we used in fact two laser systems; one with a small bandwidth for spectroscopic information, and another with a large bandwidth for the creation and detection of the wave packet. Both the laser and the vacuum system will be described in this section.

The vacuum system consists of a vessel with a background pressure of 2×10^{-7} mbar, in which a lens ($f=16$ cm) focuses the beam in a metal box. The box (see also Fig. 4) contains two condenser plates creating a homogeneous electrical field. The free electrons formed in the focus are extracted by the electrical field in the direction of the upper plate. In this plate a grid is placed through which all the electrons can reach a set of channel plates. The signal of the channel plates is amplified and averaged on a digital scope. After averaging (typical 500 shots) the signal is sent to a personal computer. In order to minimize the detection of electrons created after the pulse sequence by slow processes like collisions, we used a small time gate of 30 ns. Near the focus region the light crosses a diverging beam of rubidium coming out of a tube connected to an oven.

For the frequency-resolved experiments, we used a ns dye laser (bandwidth 0.08 cm^{-1}) pumped by the frequency doubled output of a Q-switched Nd:YAG (yttrium aluminum garnet) laser (10-Hz repetition rate). The output of the dye laser is 10 mJ ($\sim$600 nm) of which only a small part was used.

In order to create pulses with a large bandwidth the following system was used. A mode-locked Ar^+ laser (0.6-W output, 80-MHz repetition rate) synchronously pumps a linear dye laser. The dye laser is tunable around $\lambda=600$ nm. The duration of the pulses is measured with a real-time scanning autocorrelator to be 5 ps. These pulses are amplified in a three-stage dye amplifier, pumped by the second harmonic of a Q-switched Nd:YAG laser (20-Hz repetition rate). The duration of the 500-μJ amplified pulses was measured to be 7 ps.

Two kinds of experiments were performed: frequency scans for the determination of the positions of the eigenstates of the rubidium atom in the electrical field, and pump-probe scans to measure the time-dependent ionization probability. For the frequency scans a small part of the ns-dye-laser beam was led into the vacuum system. The measured photoelectron yield as function of the wavelength gives the eigenstates of the atom. For the pump-probe experiments the beam of the ps-laser system was led into a Michelson-like setup. Each pulse was divided by a beamsplitter (50-50), reflected on a mirror, and sent back to the beamsplitter. In order to create a variable delay between the two pulses, one of the mirrors was placed on a translation stage. The interference fringes of the two pulses continued over 4 ps, indicating that the pulse was about two times bandwidth limited. The pulse sequence coming out of the Michelson setup was led into the vacuum system. In this way the ionization probability can be measured as a function of the time delay between the pump and the probe pulse.

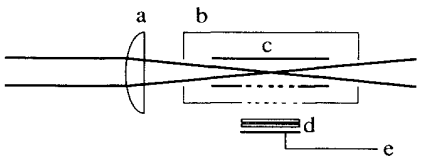

FIG. 4. Part of the experimental setup: (a) $f=16$ cm lens; (b) box in which the laser beam is focused; (c) condenser plates; (d) channel plates; and (e) electron signal.

V. RESULTS

In this section we will present the experimental results: the frequency scans over the Stark map; the influence of ac Stark shift; the pump probe experiment in which the wave packet is measured, and the experimental results with the theoretical calculations.

In Sec. I we used $\Delta E=3Fn$ for the spacing between neighboring k states in hydrogen. For rubidium, which was used in the experiments, this is not fully correct, since the spin-orbit coupling and the quantum defect are missing. More accurate calculations on the positions of the energy levels of rubidium have been made by Zimmerman *et al.*[9] In these calculations the spin-orbit coupling and the quantum defect are incorporated. We measured the resonances of the k states within one manifold by (2+1)-photon ionization. A wavelength scan was made over the $n=14$ manifold of rubidium. The applied electrical field was 2120 V/cm. From the results (Fig. 5) we find a spacing of 4.7×10^{-4} eV, which is in reasonable agreement with the $3Fn$ value of 5.3×10^{-4} eV. Although the spacing of neighboring states differs from the $3Fn$ value, the deviation is small and the approximation is good.

We are interested in the behavior of an atom placed in a dc electrical field, but there may be also some effects due to the ac electrical field of the laser. In an intense laser field high-lying Rydberg states shift as the threshold[15] if the photon energy is large compared to the spacing between the resonances. In first order a high intensi-

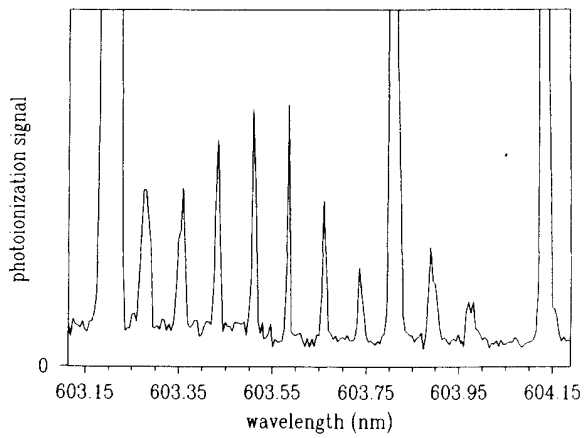

FIG. 5. Measurement of the resonances by a wavelength scan of the $n=14$ manifold with an electrical field of 2120 V/cm.

ty would lead to a shift of the whole manifold, keeping the individual k members on the same relative position. In the case of a constant spacing this shift will not influence the oscillation time of the parabolic wave packet. This is in contrast to the radial wave packet, where the spacing is not constant and a shift would lead to another oscillation time. We can estimate the shift of a manifold by measuring the shift of the threshold. This is done by measuring the photoelectron yield of the two-photon ionization of rubidium as a function of the wavelength for different light intensities. The applied static field strength was 1238 V/cm leading to a classical threshold around $n=23$. A homogeneous part of the laser beam is selected by a pinhole. Due to the large f/D ratio of 50 used, the spherical aberration is small and the spatial intensity distribution in the focus can easily be calculated. As a result of the smooth temporal structure (measured by the autocorrelation function) and the known spatial structure of the laser beam, we can calculate the maximum intensity in the focus rather accurately. For the lowest intensity we see (Fig. 6) a sharp increase of the ionization probability for wavelengths shorter than the classical threshold wavelength of $\lambda=597.45$ nm. By increasing the intensity the threshold shifts towards lower energies. For the three high-intensity measurements we calculated a decrease in energy difference in rubidium between the ground state and the threshold of 1.0 meV/(10^{11} W/cm^2). The threshold shifts with the quiver energy $E^2/4\omega^2$ towards higher energies. Apparently, the ground state shifts upwards with a larger amount to realize an overall decrease of the binding energy. The shift of the ground state ($5s$) is dominated by the interaction at the one-photon level with the $5p$ state.

In the actual pump-probe experiments the intensity never exceeded 10^9 W/cm^2 leading to a shift of 0.01 meV.

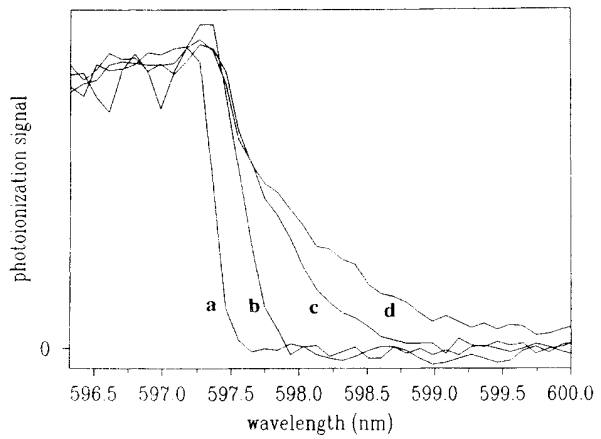

FIG. 6. The measured ac Stark shift of the classical ionization threshold for different intensities. At low intensities [(a) $I<1.0\times10^{10}$ W/cm^2] the ionization probability drops for wavelengths larger than the classical threshold for rubidium: $\lambda=597.45$ nm. The wavelength corresponding to the threshold increases with increasing intensity: the binding energy decreases for higher intensities. The lines are measured with the following peak intensities: (b) $I=9.8\times10^{10}$ W/cm^2; (c) $I=2.8\times10^{11}$ W/cm^2; (d) $I=4.2\times10^{11}$ W/cm^2.

This shift is small compared with the spacing of the coherently excited states (larger than 0.10 meV) and with the laser bandwidth ($\sim$0.50 meV). Therefore we can neglect effects due to the intensity of the laser field.

The time dependence of the ionization was measured with the pump-probe setup described in Sec. IV. Both the applied field and the excited Rydberg manifold have to be chosen. In order to avoid superposition of different n states (as in the radial wave packet) the selected n state cannot be too high: $n<35$ for the used pulse duration. Furthermore, we must avoid mixing of neighboring n manifolds, so the electrical field should be smaller than the n-mixing value: $F_n=\frac{1}{3}n^5$. A complicating factor is the quantum defect of rubidium. Starting from the ground state ($5s$), two-photon absorption leads mainly to population of the d state. Due to the quantum defect ($\delta_l=1.347$) the d state lies at $\frac{1}{3}$ between two succeeding manifolds in the zero field situation. In order to mix the population from the d state into the manifold, the electrical field must be larger than about half of the n-mixing value. The population of the manifold was checked by frequency scans over the manifold with the narrow-bandwidth laser.

We will present three experiments with different selected manifolds and applied fields (Fig. 7). For all the results the signal caused by direct three-photon ionization of both individual pulses has been subtracted. The polarization of the laser was chosen to be parallel with the dc electrical field, leading to the selection rule $\Delta m=0$. Since m of the ground state is zero, m is zero for all the states.

In the first [Fig. 7(a)] experiment the $n=21$ manifold was excited while the applied field was 390 V/cm ($F_n=420$ V/cm). Enhancement of the ionization can clearly be seen at $\Delta t=32$, 64, and 93 ps, in good agreement with the value predicted by Eq. (1): 31.8 ps. This measurement shows the periodic oscillations of a parabolic wave packet. Around zero delay there is a large peak in the ionization signal. This is the result of the so-called coherent spike in the light intensity, due to the interference between the two beams of the Michelson interferometer. For a third-order process the signal in the coherent spike can be 32 times higher than the sum of the signal of the individual beams. This enhancement is not realized in the experiments due to fluctuations of the length of the arms of order λ, and because the spatial overlap of the foci was not perfect.

In the second experiment the $n=19$ manifold was selected while the applied field was 645 V/cm ($F_n=692$ V/cm). Again the peaks in the ionization yield are in good agreement with the predicted value of 21.3 ps. An important feature of Fig. 7(b) is the large number of observed oscillations of the wave packet, indicating that the dispersion is indeed much smaller than in the case of the radial wave packet. Nevertheless, for longer delay times the signal decreases and the modulation becomes weaker. The decrease in signal is due to decrease of the laser intensity during the scan (2 h). The decrease in modulation shows that there is some dispersion of the wave packet: the spacing of the different k states is not exactly constant.

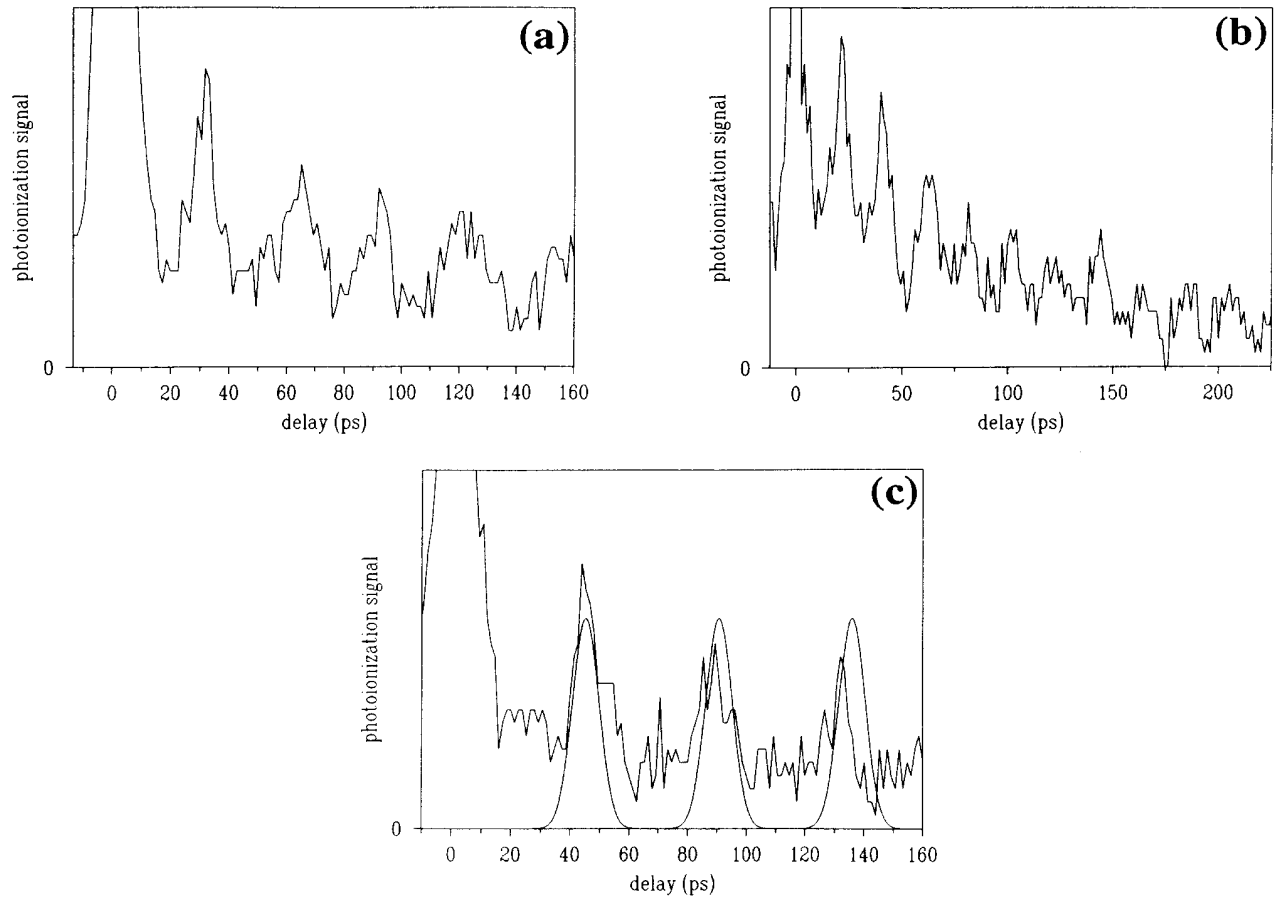

FIG. 7. The pump-probe ionization signal as a function of the time-difference between the two pulses. (a) The $n=21$ manifold was excited and the field strength ($F=420$ V/cm) leads to an oscillation time of 31.8 ps. The periodic peaks in the ionization signal for increasing delay reflect the oscillation of the parabolic wave packet. (b) The $n=19$ manifold was excited and the field strength ($F=645$ V/cm) leads to an oscillation time of 21.3 ps. Ten oscillations of the wave packet can be observed, indicating that the dispersion is low. (c) The $n=23$ manifold was excited and the field strength ($F=248$ V/cm) leads to an oscillation time of 45.8 ps (noisy line). Furthermore the calculated ionization probability is plotted (smooth line). The only fitted parameter in the calculations is the vertical scale.

The results of the third experiment are shown in Fig. 7(c). In an electrical field of 248 V/cm ($F_n=266$ V/cm) the $n=23$ manifold was excited. In this case the oscillation time (45.8 ps) is much longer than the pulse duration: there is a flat background between the peaks. For the given experimental conditions we also calculated the time-dependent ionization probability according to Eq. (7). The coherent spike is not taken into account, since the calculation does not incorporate small delay times. Although the calculation of the l population was done for hydrogen, there is good agreement with the experimental results. Note that the only fitted parameter is the absolute value of the photoionization signal, since this experiment gives relative values. In the experiment an unpredicted decrease of the signal can be observed. This is again due to a decrease of the laser intensity during the scan, which was not incorporated in the calculations.

VI. CONCLUSIONS

We have coherently excited a number of parabolic states, all from one n manifold, with a short laser pulse. The resulting wave function is not a stationary one, due to the different energies of the parabolic states in an electrical field. The wave packet hardly disperses, since the energy differences between the involved eigenstates are almost constant. Both the oscillation period and the reduced dispersion are shown experimentally by measuring the fraction of the wave function near the atomic core, as a function of time. The calculation of the l populations is done for hydrogen, whereas the experiment is done with rubidium. The role of the quantum defect and the spin-orbit coupling is not incorporated. Nevertheless, there is a good agreement between the calculations and the experimentally measured photoionization probability.

ACKNOWLEDGMENTS

We would like to thank W. Sandner, T. F. Gallagher, H. G. Muller, H. J. Bakker, and M. Pont for many helpful discussions. This work is part of the research program of the Stichting voor Fundamenteel Onderzoek der Materie (Foundation for the Fundamental Research on Matter) and was made possible by the financial support of the Nederlandse Organisatie voor Wetenschappelijk Onderzoek (Netherlands Organization for the Advancement of Research).

[1]E. Schrödinger, Naturwissenschaften **28**, 664 (1926).
[2]J. Parker and C. R. Stroud, Jr., Phys. Rev. Lett. **56**, 716 (1986).
[3]G. Alber, H. Ritsch, and P. Zoller, Phys. Rev. A **34**, 1058 (1986).
[4]J. A. Yeazell and C. R. Stroud, Jr., Phys. Rev. A **35**, 2806 (1987); Phys. Rev. Lett. **60**, 1494 (1988).
[5]L. D. Noordam, A. ten Wolde, H. G. Muller, A. Lagendijk, and H. B. van Linden van den Heuvell, J. Phys. B **21**, L533 (1988).
[6]A. ten Wolde, L. D. Noordam, A. Lagendijk, and H. B. van Linden van den Heuvell, Phys. Rev. Lett. **61**, 2099 (1988).
[7]A. ten Wolde, L. D. Noordam, H. G. Muller, and H. B. van Linden van den Heuvell, in *Fundamentals of Laser Interactions II*, Vol. 339 of *Lecture Notes in Physics*, edited by F. Ehlotzky (Springer-Verlag, Berlin, 1989).
[8]A. ten Wolde, L. D. Noordam, A. Lagendijk, and H. B. van Linden van den Heuvell, Phys. Rev. A **40**, 485 (1989).
[9]M. L. Zimmerman, M. G. Littman, M. M. Kash, and D. Kleppner, Phys. Rev. A **20**, 2251 (1979).
[10]D. A. Harmin, Phys. Rev. A **30**, 2413 (1984).
[11]E.g., *Beam-foil spectroscopy*, Vol. 1 of *Topics in Current Physics*, edited by S. Baskin (Springer-Verlag, Berlin, 1976).
[12]H. A. Bethe and E. E. Salpeter, *Quantum Mechanics of One- and Two-Electron Atoms* (Springer-Verlag, Berlin, 1957).
[13]D. Park, Z. Phys. **159**, 155 (1960).
[14]M. V. Fedorov and A. M. Movsesian, J. Opt. Soc. Am. B **5**, 850 (1988).
[15]S. Liberman, J. Pinard, and A. Tabel, Phys. Rev. Lett. **50**, 888 (1983).